ARTICLE

Accessible Triplet Excited States in the Photoisomerization of Allenes with Extended Conjugation

Jonathan Álvarez-García,[a] Ramón García-Lago,[a] Jose Lorenzo Alonso-Gómez,[a] Carlos Silva López*[a] and María Magdalena Cid*[a]

A series of bidentate allene- and enyne-containing ligands have been synthesized and the photochemical properties of their rhenium (I) complexes have been studied. These complexes exhibit facile isomerization of the conjugated double bonds upon ambient light exposure. Simulations unveiled a very efficient intersystem crossing and the consequent key role of the triplet states in the observed photochemistry of these substrates upon rhenium (I) complexation.

Introduction

One of the goals of our research group is the synthesis of chiral, shape-persistent macrocycles and, in order to achieve systems with improved sensing capabilities, we have taken advantage of the inherent 90° twist of allenes to build scaffolds with interesting 3D geometries and promising photophysics.[1,2] In the course of this research we observed *P*/*M*-photoisomerization of allenyl compounds,[3] especially, when diethynylallene (**DEA**) moieties were conjugated with electron-rich groups as anthracene[4] **A** or amines[5] **B**. We reported the same phenomenon with an electron-deficient fragment such as pyridine (**C**) due to high ring-strain, which seemed to be the driving force in this process (Scheme 1). Actually, when the spacer was replaced by a longer linker, like bipyridine, no photoisomerization was observed.[6]

Late-transition metal complexes of heterocyclic nitrogen compounds, such as pyridine and bipyridine, represent an important class of chromophores with interesting properties in the field of photochemical devices,[7–12] among them, several Re(I) complexes[13] undergo a rich variety of photophysical phenomena due to accessible π-π* and metal-ligand charge transfer (MLCT) transitions. With this in mind, we hypothesized that the coordination of late-transition metals by our allenophanes could give rise to remarkable spectroscopic features with broad applicability in the field of sensing. Nevertheless, photoisomerization can also be expected upon transition metal complexation[14] as reported in a series of Re(I) complexes bearing photoisomerizable groups.[15–21]

The role of the Re-based MLCT has been theoretically described as the necessary vehicle for an intersystem crossing (ISC) from a singlet to a triplet π-π* excited state.[22–24]
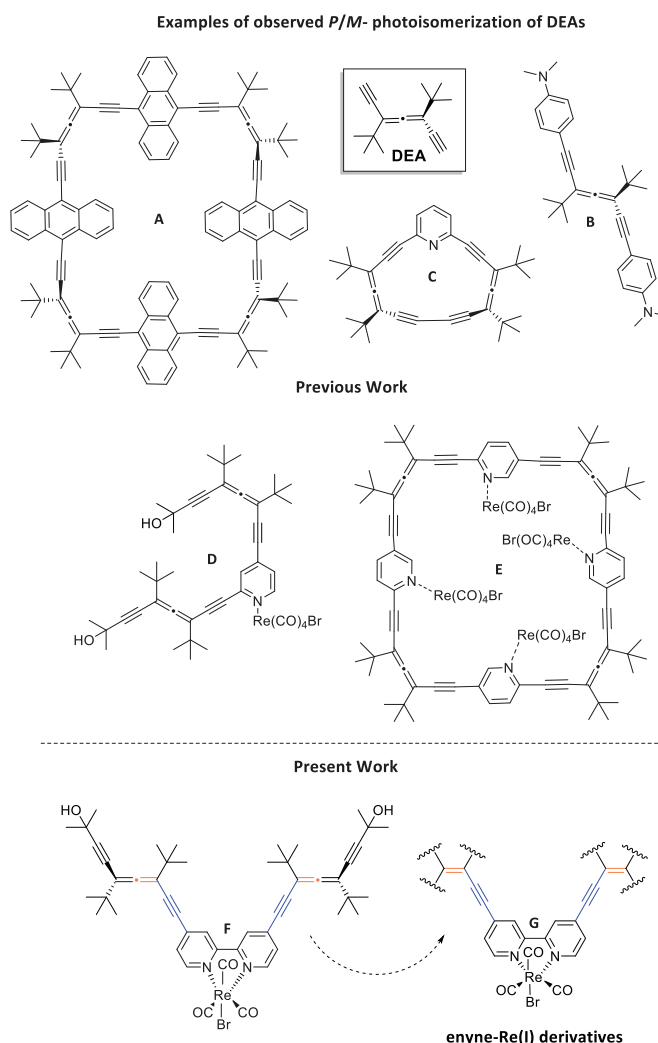
[a] Departamento de Química Orgánica, Universidade de Vigo, Edificio de Ciencias Experimentais, Campus Lagoas-Marcosende, 36310, Vigo, España
E-mail: mcid@uvigo.gal, carlos.silva@uvigo.es

Scheme 1 Top: Examples of some compounds reported in the literature that undergo photoisomerization of DEA units and pyridine bearing DEAs as ligands in complexes of the type [Re(CO)₄LBr]. Bottom: Schematic representation of allenyl and different enyne-Re(I) derivatives reported in this work.

Since we are interested in using allenyl macrocyclic systems with intense chiroptical responses, conformational and configurational stability are mandatory. In this context, we aim to examine the photostability of DEAs in late transition metal organometallic complexes. Early studies showed how racemic 2,4- **D** and 2,5-DEA-functionalized pyridines as well as pyridoallenophanes **E** could be used as suitable ligands (L) in tetracarbonylrhenium complexes of the type [Re(CO)$_4$LBr] (Scheme 1). These complexes were fully characterized with the synergy of experimental and computational methods, and the lowest-energy absorption band was assigned to a metal-ligand-to-ligand charge-transfer transition.[25] Taking a step forward in the study of this type of metal complexes, we decided to use enantiopure 4,4'-DEAs featuring 2,2'-bipyridines as ligands. We expected that conjugation beyond the bipyridine ligand would facilitate the appearance of MLCT transitions. With the goal of studying the contribution of the different structural moieties of allenylynes **F**, we have also truncated the group into enynes **G** to infer the role of the cumulated unit in the photophysics of these compounds (Scheme 1, bottom). Therefore, here we present the preparation and the study of the photostability under ambient conditions of allenyl and different enyne-Re(I) derivatives in which the chromophoric and the photoisomerizable groups are not independent.

Results and discussion

Synthesis of the Re(I) complexes and study of their photochemical properties

The formation of the Re(I)-complex from bipyridine (*P*)-**1a**[‡] via treatment with Re(CO)$_5$Br in THF at 60 °C (Fig. 1 top) became evident in the ^{1}H NMR spectra since the aromatic signals of the bipyridine unit experienced a significant downfield shift due to the inductive effect of the metal. Re(I)-**1a** has a bright orange color in solution and in the solid state that corresponds to an absorption band in their UV-vis spectra around 400 nm. This band is not present in the starting ligand and can be attributed to a metal-ligand charge transfer transition (Fig. 1 bottom). The two highest energy bands are red-shifted in the Re(I) complex (270 and 330 nm) from the related bands found in the free ligand (260 and 304 nm, respectively) which are ascribed to intraligand (IL) transitions. The formation of the complex was also confirmed by X-ray crystallography. The crystal structure showed that the complex adopted an octahedral arrangement around the rhenium(I) center. The ligand (*P*)-**1a** is coordinated to the metal by both bipyridine nitrogen atoms in a *cis* manner, while the three carbonyl ligands are disposed in a facial configuration. The sample crystallized in the chiral space group I2$_1$2$_1$2$_1$ and the absolute configuration of the allenyl-motif was corroborated.[26]

With complex Re(I)-**1a** at hand, we decided to study its photostability. Since a hypothetical photoisomerization process would generate stereoisomeric mixtures, we decided to follow the process using circular dichroism (CD). To do so, once the ligand exchange reaction was finished, the reaction mixture
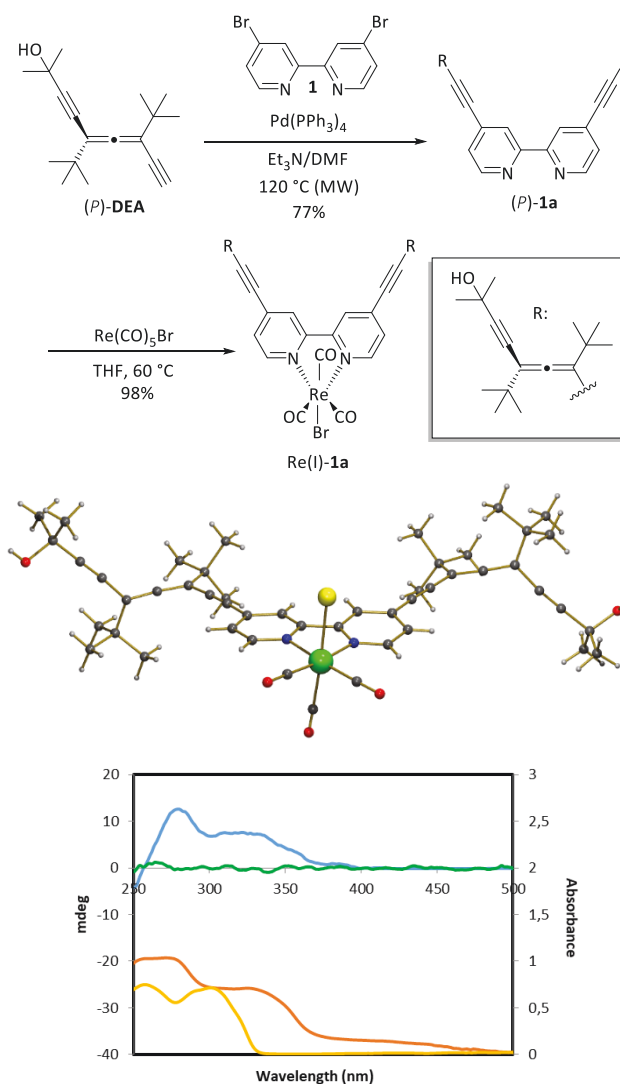

Fig. 1 Schematic representation of the synthesis of Re(I)-**1a** (top) and its crystal structure (middle). Hydrogen atoms were omitted for clarity. Bottom: UV-vis spectra of ligand (*P*)-**1a** (chloroform, 2.4 x 10^{-5} M, yellow line) and Re(I)-**1a** (orange line) and CD spectra before (blue line) and after 15 min of sunlight exposure (green line) of complex Re(I)-**1a** (chloroform, 2.4 x 10^{-5} M).

was brought to dryness, taken-up in chloroform and its CD-UV-vis spectra recorded without further purification. By avoiding exposing Re(I)-**1a** to sunlight, we managed to record its CD spectra indicating that racemization was successfully avoided during the ligand exchange reaction (Fig. 1 bottom, blue line). However, when the same solution was exposed to sunlight for only 15 min, chirality was lost as indicated by the complete disappearance of its CD signals (Fig. 1 bottom, green line). In contrast, the free ligand (*P*)-**1a** needed more than 36 h of exposure to sunlight to lose a small fraction of its chiral integrity (See Fig. S3 in the ESI). A similar phenomenon was described by Diederich's group, where the complexation of Zn(II) by a DEA functionalized phenanthroline and its subsequent exposure to sunlight produced its racemization.[27]

To study the effect of substitution of the DEA motif on the photoisomerization process, we considered using enynes as structural probes and, in doing so, a series of new ligands were prepared. Most of them were obtained in a single step that
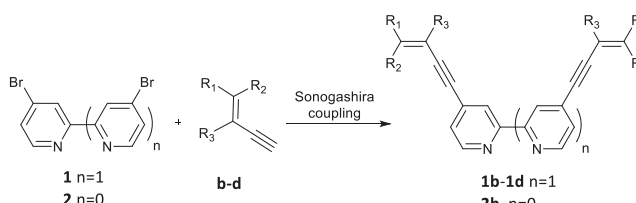
consisted of a Sonogashira reaction between 4,4'-dibromo-2,2'-bipyridine (**1**) or 4-bromopyridine (**2**) and the corresponding enyne.[27] The results, as well as the conditions used, are summarized in Table 1.[‡] On the other hand, ligand (*E*)-**1b** was obtained quantitatively from (*E*)-**1c** by deprotection of silyl ethers by treatment with TBAF in THF at room temperature for 15 min. Additionally, Dess-Martin oxidation of diol (*Z*)-**1b** in THF rendered dialdehyde (*Z*)-**1e** in a 52% yield (See the ESI for details).

With the ligands at hand, the Re(I) complexes were prepared by a ligand-exchange reaction from Re(CO)$_5$Br in THF, heating the mixture to a temperature between 60-70 °C in the dark (Table 2). As in the case of the allenyl complex, most of the complexes (Re(I)-(**1b**-**1d**)) have an orange coloration and a new absorption band in their UV-vis spectra at around 400 nm. In the case of complex Re(I)-(*Z*)-**1e** (red color), this band is further red-shifted (435 nm) as a consequence of the presence of the conjugated aldehyde groups, which seem to lower the energy of the π* orbital and consequently decrease the HOMO-LUMO gap. On the opposite side, complex Re(I)-(*Z*)-**2b** presents a faint yellow color probably due to the reduced conjugation in this pyridyl system compared to the bipyridyl analogues.

Surprisingly, some loss of configurational integrity of the double bond of the enynes was observed during the first attempts to carry out the complexation reaction at ambient light. As an example, when we used allyl alcohols (*Z*)-**1b** or (*E*)-**1b** as starting materials, we found that Re(I)-**1b** was always obtained as a 5:1 isomeric ratio. NOESY experiments made possible to establish that the major compound in this mixture was Re(I)-(*Z*)-**1b**. (See Figure S22 in the ESI).

To help us understand this process, the ligand exchange reaction with (*E*)-**1b** was set up in a sealed NMR tube and kept in the dark. It could be observed in the ^{1}H NMR spectra how, at 60 °C, the free ligand gradually disappeared, being the formation of the Re(I) complex practically complete in 3 hours.
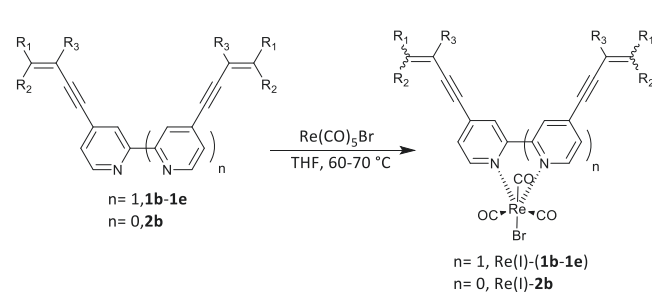
Table 1 Summary of the ligands synthesized by a Sonogashira reaction

Entry	Aryl	Enyne	R$_1$	R$_2$	R$_3$	Product	Yield (%)
1	**1**	(*Z*)-**b**	H	CH$_2$OH	Me	(*Z*)-**1b**^{a}	78
2	**1**	(*E*)-**c**	CH$_2$OTMS	H	Me	(*E*)-**1c**^{a}	90
3	**1**	(*E*)-**d**	CH$_2$OH	Me	H	(*Z*)-**1d**^{b}	77
4	**2**	(*Z*)-**b**	H	CH$_2$OH	Me	(*Z*)-**2b**^{c}	54

^{a} Pd(PPh$_3$)$_2$Cl$_2$ (5% mol), CuI (5% mol), iPrN$_2$H/THF, 4h, 40 °C. ^{b} Pd(PPh$_3$)$_4$ (5% mol), CuI (10% mol), pyrrolidine, 21h, rt. ^{c} Pd(PPh$_3$)Cl$_2$ (5% mol), CuI (5% mol), Et$_3$N, 20 h, rt.

Table 2 Summary of the Re(I) complexes synthesized by a ligand exchange reaction

Entry	Ligand	R$_1$	R$_2$	R$_3$	Product^a	Yield (%)^b
1	(*Z*)-**1b**	H	CH$_2$OH	Me	Re(I)-(*Z*)-**1b**^{a}	33
2	(*E*)-**1b**	CH$_2$OH	H	Me	Re(I)-(*E*)-**1b**^{a}	100*
3	(*E*)-**1d**	CH$_2$OH	Me	H	Re(I)-(*E*)-**1d**^{a}	75
4	(*Z*)-**1e**	H	CHO	Me	Re(I)-(*Z*)-**1e**	37
5	(*Z*)-**2b**	H	CH$_2$OH	Me	Re(I)-(*Z*)-**2b**^{c}	32

General conditions: A mixture of Re(CO)$_5$Br (1 equiv) and the corresponding ligand (1 equiv) was heated (60–70 °C) in the dark in dry THF between 5 and 16 hours under an Ar atmosphere. ^{a}Although amber material was used, some sunlight-driven isomerization could not be avoided. ^{b} Isolated yield; ^{c} 2 equiv of ligand (*Z*)-**2b** were used and incorporated into the complex.*NMR yield.

At this point, no isomerization was observed and only Re(I)-(*E*)-**1b** was present (See Fig. S13 in the ESI). However, if the solution was exposed to sunlight, photoisomerization occurred at room temperature reaching the photostationary state in 5 h and in which the Re(I)-(*Z*)-**1b** isomer was again the major product. The graphical representation of the change in the concentration of both isomers over time showed how the disappearance of Re(I)-(*E*)-**1b** coincided with the appearance of Re(I)-(*Z*)-**1b** in the same proportion. We therefore hypothesized that the photoisomerization reaction would correspond to an equilibrium in which both the direct and inverse reactions would be unimolecular processes. The rate constants could be calculated obtaining k_1=0.54 s^{-1} and k_{-1}=0.11 s^{-1} (Fig. 2).

The course of the reaction with ligands (*Z*)-**1e** and (*Z*)-**2b** was also followed by ^{1}H NMR (See Fig. S28 and S31 in the ESI). Keeping the NMR tube in the dark, complexes Re(I)-(*Z*)-**1e** and Re(I)-(*Z*)-**2b** were obtained as the only products and they could also be isolated (Entries 4 and 5 respectively, Table 2). As it happened previously, when both complexes were exposed to sunlight, their photoisomerization was activated. Re(I)-**1e** reached the photostationary state in 5 h, with a 5:1 isomeric ratio, being Re(I)-(*Z*)-**1e** the major one. Re(I)-**2b** reached the photostationary state in just 1 hour, with the ratio of isomers being 1:0.8 and Re(I)-(*Z*)-**2b** as the major isomer.
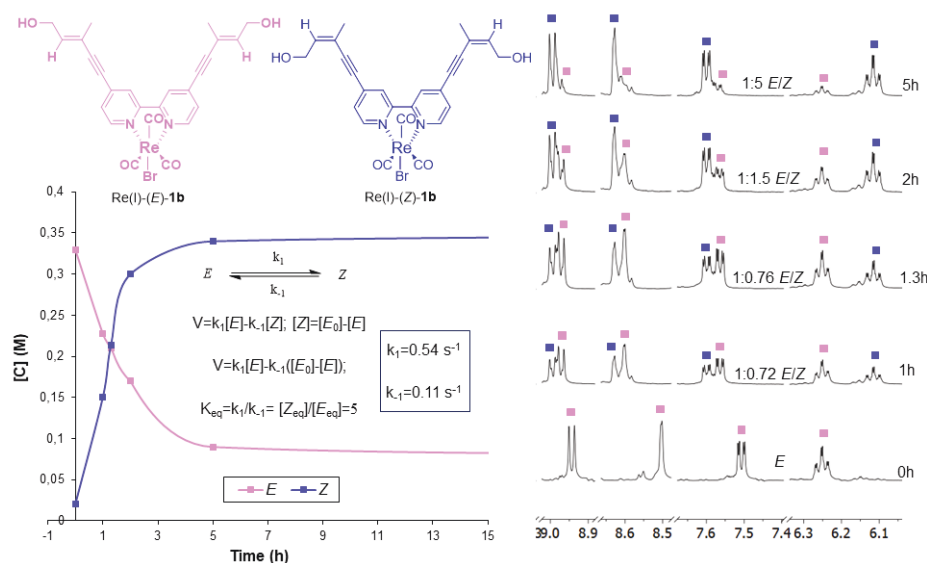
Fig. 2 Left: Representation of the change in the concentration of both Re(I)-(*E*)-**1b** and Re(I)-(*Z*)-**1b** over time; rate constants calculation. Right: Photoisomerization reaction of Re(I)-(*E*)-**1b** followed by ^{1}H NMR.

Computational study on the mechanism of the photochemical isomerization

To explain our results, we decided to carry out a detailed computational exploration of the ground and lowest excited states for these systems.[29] Simulations were carried out with the PBE0 density functional by using the double-ζ quality 6-31+G(d,p) basis set for the light atoms (C, N, O and H) and the LANL2DZ electron core potential and its associated basis set for the Re atom.[30] Further details regarding the computational methodology can be found in the ESI.
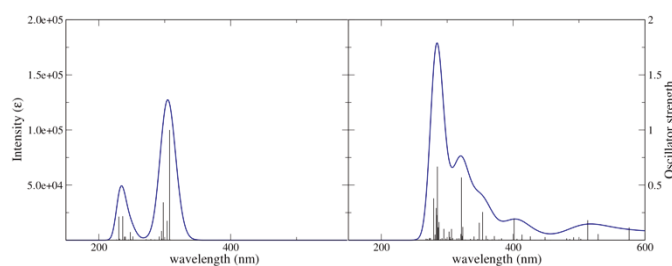

Fig. 3 Simulated UV/vis spectra for free ligand (Z)-1e (left) and complex Re(I)-(Z)-1e (right).

An initial assessment of experimentally recorded and simulated UV-vis absorption spectra of the free bipyridine systems and the corresponding Re complexes (Fig. 3 for illustrative examples, data for other systems in the ESI) confirmed our hypothesis that the overall effect of the Re complexation is a significant reduction of the energy requirements to populate a number of excited states that are only available beyond the 300 nm regime in the isolated ligand. Namely, a general red shifting was observed upon complexation, and an additional band appeared at wavelengths significantly lower than those observed in the free ligand (at around 400 nm in most cases).

In particular it seems that this band appearing at about 400 nm in the Re complex may not only be responsible for the colour observed in these complexes, but it could also have a relevant role in their photochemistry.[31]

In order to explore with more detail this possible effect of the complexation of Re onto the photochemical behaviour of our substrate, we completed a full scan of the isomerization process via partial geometry optimizations (with a single degree of freedom constrained, the CCCC dihedral angle associated to the double bond isomerization). The thus obtained energy plots computed for the isolated organic substrate **1a** and Re(I)-**1a** revealed interesting differences (Fig. 4). The free ligand **1a** (Fig. 4 top) showed a cluster of forbidden transitions (S_0->T_n) around 3.0 eV and a more probable S_0->S_1 transition just above 4 eV.

The S_1 electronic state is bright, with a rather large associated oscillator strength (ca. 1.4) but it is only accessible by employing incident radiation of 310 nm or lower wavelength. Upon Re complexation the picture differs significantly. Singlet transitions become less energy demanding and are clustered together with low energy triplet states. This situation allows for a symmetry permitted transition into a bright singlet state and an efficient intersystem crossing (ISC) into a nearby triplet.

Additionally, transitions S_0->S_1 and S_0->T_1 display a clear metal-to-ligand-charge transfer character as depicted in Fig. 4 (bottom). In this regard, since we studied the entire profile, we also have a reasonable estimate for the cost of the transition state on the excited state surface. In this case, for T_1, the activation barrier would be 0.5 eV (11.5 kcal/mol) which seems easily surmountable at room temperature considering that photoexcitation usually implies strongly excited vibrational states at the arriving surface. This barrier contrasts with around 1.5 eV for isomerization in S_0 and S_1, suggesting again that the eventual photoisomerization process is likely to proceed only after a singlet to triplet ISC event.
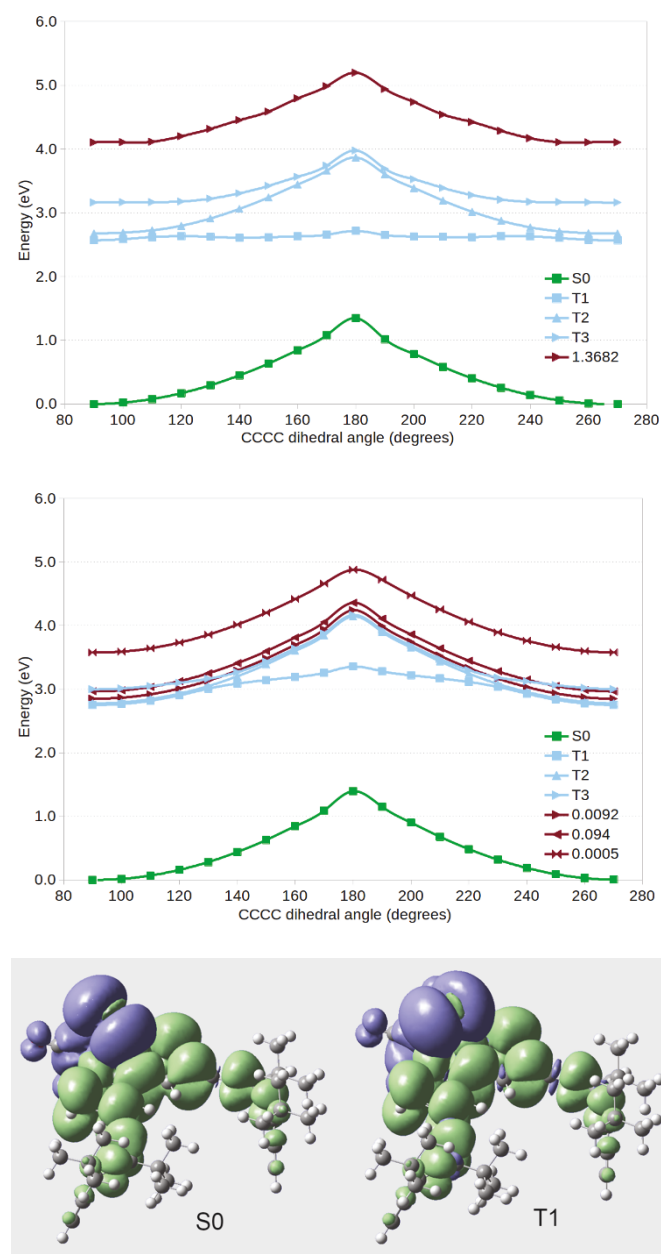
according to the computed barriers, and considering the short times required for internal conversion, relaxation to the S1 state is expected. Once at the lowest singlet excited state an intersystem crossing event to the triplet opens the way to a facile *Z-E* isomerization. Our simulated absorption spectra qualitatively suggests that the *E* isomer is more readily excited and thus converted into its *Z* isomer and should be found in relatively lower concentration upon photo-stationary equilibrium is reached (see the SI).
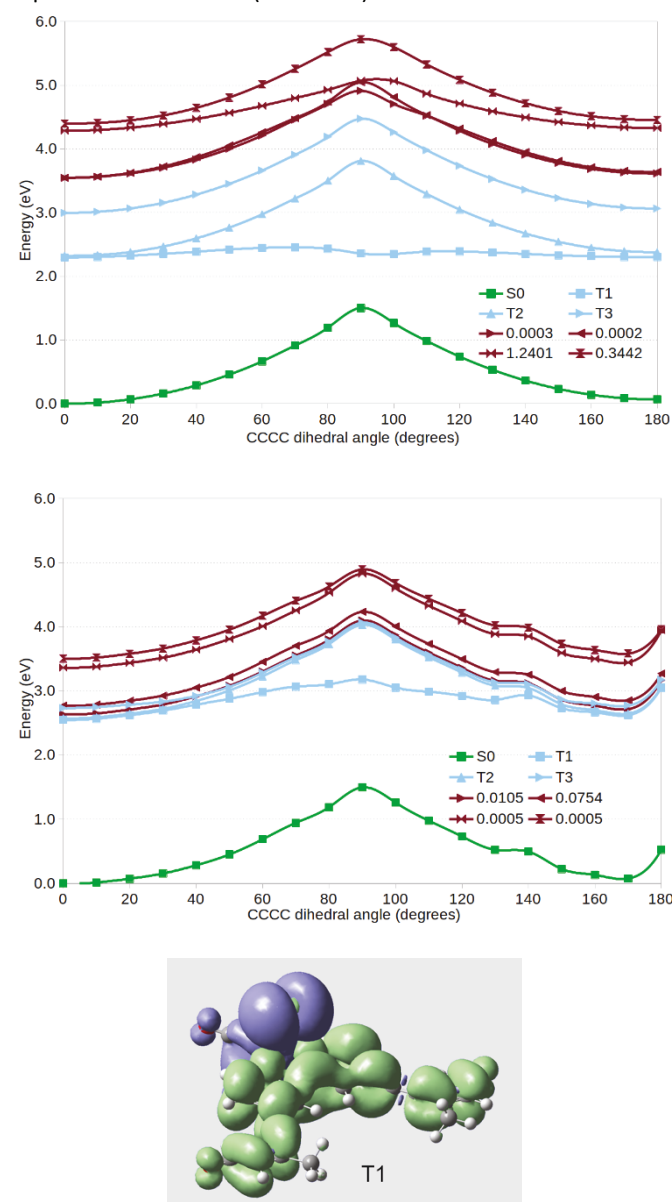

Fig. 4 Relative energies for ground (green) and the lowest triplet (cyan) and bright singlet (red) states (in eV) during allene isomerization as a function of the CCCC dihedral angle in degrees for **1a** (top) and Re(I)-**1a** (center). Oscillator strengths for the singlet states (legend values for the red lines) were computed from the ground state at the starting geometry. Plot of the electronic density difference for S1 and T1 (bottom) for Re(I)-**1a**. Negative values of electron density in purple and positive ones in green.

In order to draw a line of argument for the isomerization of double bonds we run the same procedures for eninal **1e** and Re(I)-**1e** (Fig. 5). The obtained results for **1e** rendered a similar situation to **1a** but with a larger number of accessible states in both the singlet and the triplet configuration. Again, the lowest triplet state provides a path for the *Z/E* isomerization with an energy barrier of about 0.5 eV. Experimentally, the observed photo-stationary equilibrium for Re-enynal **1e** is reached at a 5:1 mixture of *Z/E* isomers. This combined experimental and computational data suggests that initially the system is excited via the red-shifted band at about 350 nm since it is much brighter than the new lower energy band at 400 nm. However,

Fig. 5 Relative energies for ground (green) and the lowest triplet (cyan) and bright singlet (red) states (in eV) during allene isomerization as a function of the CCCC dihedral angle in degrees for **1e** (top) and Re(I)-**1e** (center). Oscillator strengths for the singlet states (legend values for the red lines) were computed from the ground state at the starting geometry. Plot of the electronic density difference for T1 (bottom) for Re(I)-**1e**. Negative values of electron density in purple and positive ones in green.

Each of these allenes/enynes present in the corresponding ligand can undergo independent photochemical events. Therefore, it is necessary to take into account the possibility of the formation of the (*P*,*M*) stereoisomer, in the case of ligand **1a**, and the (*Z*,*E*) stereoisomers for the remaining ligands. The

appearance of Re(I)-(*P*,*M*)-**1a** would also cause the disappearance of the CD signal of Re(I)-(*P*,*P*)-**1a** because it is a meso form.

On the other hand, the isomerization of the enynes was followed by means of ^{1}H NMR and apparently only two compounds coexist once the photostationary state was reached. A possible explanation for this observation is that even if the hypothetical formation of the (*Z*,*E*) isomer occurs, its chemical shift must overlap with that of the (*Z*,*Z*) and (*E*,*E*) isomers. In order to test the plausibility of this hypothesis, the chemical shifts of the three isomers of Re(I)-**1e** were computationally simulated (Fig. 6) showing that indeed, the formation of (*Z*,*E*) would not be observable via NMR as its chemical shifts would coincide with those stemming from the other two.
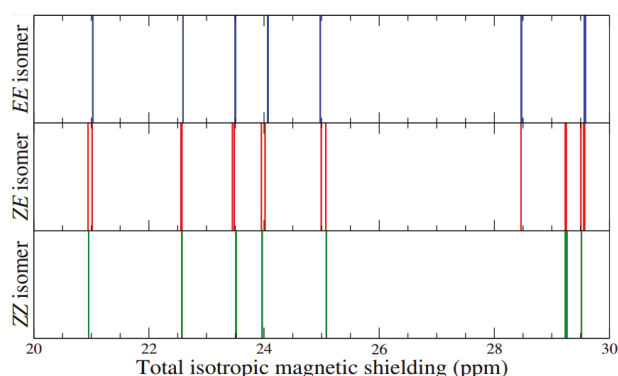

Fig. 6 Total isotropic magnetic shieldings (in ppm) computed for ^{1}H nuclei in the (*EE*), (*ZE*) and (*ZZ*) isomers of Re(I)-**1e**.

With these results at hand, we were set to forge an explanation for the fast isomerization of anthracenoallenophane **A** and dimethylanilinyllallene **B** (Scheme 1) in the presence of ambient light and find out if the isomerization follows the same mechanism. We had ascribed the fast photoisomerization of **A** to the triplet sensitizing ability of the anthracene moiety[4] and Diederich has reasoned that the fast isomerization of dimethylaniline substituted allenes is based on the donating ability of the dimethylamino group.[5] Now calculations run following the same protocol as for **1a**, rendered very facile isomerization processes also via triplet excited states once a seemingly facile ISC event occurs (Fig. 7).

Conclusion

A series of Re(I) complexes with DEA- and enyne-containing ligands have been successfully synthesized and characterized. Upon exposure to ambient light and temperature, the complexes undergo photoisomerization which could be easily monitored by circular dichroism or NMR spectroscopy. The mechanism of the photochemical event observed was investigated by calculations of the potential energy profile in the ground and excited states of both complexes and free ligands, taking into account the CCCC dihedral angle associated to the double bond or the allene. Complexation acts as a pathway for a very efficient ISC, allowing a triplet excited state to be reached where the activation energy for the isomerization

process is considerably lower than in the singlet state. So, we have clarified in depth the role of the rhenium(I) ion in photoisomerization processes that will help in designing devices for technological applications thanks to the tunable photochemical and photophysical properties of pyrido-Re(I) complexes.
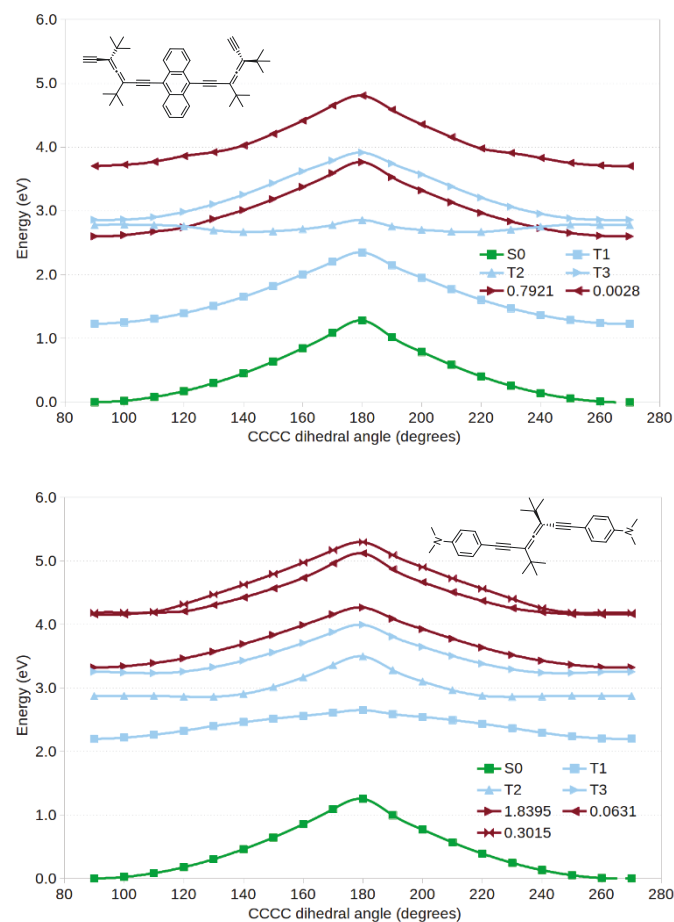

Fig. 7 Relative energies for ground (green) and the lowest triplet (cyan) and bright singlet (red) states (in eV) during allene isomerization as a function of the CCCC dihedral angle in degrees for **A** (top) and **B** (bottom) in the absence of metal complexation. Oscillator strengths for the singlet states (legend values for the red lines) were computed from the ground state at the starting geometry.

Author Contributions

JAG, RGL and JLAG contributed with investigation and methodology. JAG, CSL and MMC wrote the first draft and also edited final versions. CSL dealt with formal analysis and MMC with project administration and conceptualization issues.

Conflicts of interest

There is no conflict to declare.

Acknowledgements

Notes and references

‡ It should be noted that bipyridine **1a** is composed of two homochiral DEA units, in the same way that the bipyridines **1b** to **1e** contain two enynes with the same configuration. For clarity, during the course of this work we abbreviated the configuration of the allenes (*P,P*) as (*P*) and that of the enynes (*Z,Z*) or (*E,E*) as (*Z*) or (*E*), respectively.

1   S. Míguez-Lago and M. M. Cid, *Synthesis*, 2017, **49**, 4111–4123.

2   I. R. Lahoz, A. Navarro-Vázquez, A. L. Llamas-Saiz, J. L. Alonso-Gómez and M. M. Cid, *Chem. Eur. J.*, 2012, **18**, 13836–13843.

3   M. M. Cid, M. Lago-Silva, M. G. Comesaña, O. Nieto Faza and C. S. López, *Org. Chem. Front.*, 2019, **6**, 1780–1786.

4   S. Odermatt, J. L. Alonso-Gómez, P. Seiler, M. M. Cid and F. Diederich, *Angew. Chem. Int. Ed.*, 2005, **44**, 5074–5078.

5   J. L. Alonso-Gómez, P. Schanen, P. Rivera-Fuentes, P. Seiler and F. Diederich, *Chem. Eur. J.*, 2008, **14**, 10564–10568.

6   S. Castro-Fernández, J. Álvarez-García, L. García-Río, C. Silva López and M. M. Cid, *Org. Lett.*, 2019, **21**, 5898–5902.

7   A. O. T. Patrocínio and N. Y. Murakami Iha, *Inorg. Chem.*, 2008, **47**, 10851–10857.

8   A. Bianchi, E. Delgado-Pinar, E. García-España, C. Giorgi and F. Pina, *Coord. Chem. Rev.*, 2014, **260**, 156–215.

9   V. Sathish, E. Babu, A. Ramdass, Z.-Z. Lu, T.-T. Chang, M. Velayudham, P. Thanasekaran, K.-L. Lu, W.-S. Li and S. Rajagopal, *RSC Adv.*, 2013, **3**, 18557–18566.

10   R. C. Amaral and N. Y. Murakami Iha, *Dalt. Trans.*, 2018, **47**, 13081–13087.

11   L. A. Faustino, A. E. Hora Machado and A. O. T. Patrocinio, *Inorg. Chem.*, 2018, **57**, 2933–2941.

12   R. C. Amaral, L. S. Matos and N. Y. Murakami Iha, *J. Photochem. Photobiol. A*, 2021, **418**, 113402.

13   J. R. Dilworth, *Coord. Chem. Rev.*, 2021, **436**, 213822.

14   C. Daniel and C. Gourlaouen, *Coord. Chem. Rev.*, 2017, **344**, 131–149.

15   J. Bossert and C. Daniel, *Chem. Eur. J.*, 2006, **12**, 4835–4843.

16   M. Kayanuma, E. Gindensperger and C. Daniel, *Dalt. Trans.*, 2012, **41**, 13191–13203.

17   J. Eng and C. Daniel, *J. Phys. Chem. A*, 2015, **119**, 10645–10653.

18   D. Chartrand, C. A. Castro Ruiz and G. S. Hanan, *Inorg. Chem.*, 2012, **51**, 12738–12747.

19   L. S. Matos, R. C. Amaral and N. Y. Murakami Iha, *Inorg. Chem.*, 2018, **57**, 9316–9326.

20   K. P. S. Zanoni and N. Y. Murakami Iha, *Dalt. Trans.*, 2017, **46**, 9951–9958.

21   J.-L. Lin, C.-W. Chen, S.-S. Sun and A. J. Lees, *Chem. Commun.*, 2011, **47**, 6030–6032.

22   E. Gindensperger, H. Köppel and C. Daniel, *Chem. Commun.*, 2009, **46**, 8223–8225.

23   M. Kayanuma, C. Daniel, H. Köppel and E. Gindensperger, *Coord. Chem. Rev.*, 2011, **255**, 2693–2703.

24   X. Yi, J. Zhao, J. Sun, S. Guo and H. Zhang, *Dalt. Trans.*, 2013, **42**, 2062–2074.

25   L. Alonso-Gómez, A. Navarro-Vázquez and M. Magdalena Cid, *Chem. Eur. J.*, 2009, **15**, 6495 – 6503.

26   CCDC 2113803 contains the supplementary crystallographic data for this paper.

27   O. Gidron, M. O. Ebert, N. Trapp and F. Diederich, *Angew. Chem. Int. Ed.*, 2014, **53**, 13614–13618.

28   R. García-Lago, J.-L. Alonso-Gómez, C. Sicre and M.-M. Cid, *Heterocycles* 2008, **75**, 57–64.

29   L. González, D. Escudero and L. Serrano-Andrés, *ChemPhysChem*, 2012, **13**, 28–51.

30   a) J. P. Perdew, M. Ernzerhof and K. Burke, *J. Chem. Phys.*, 1996, **105**, 9982–9985 b) C. Adamo and V. Barone, *J. Chem. Phys.* 1999, **110,** 6158 c) R. Ditchfield, W.J. Hehre and J.A. Pople, *J. Chem. Phys.* 1971, **54**, 724 d) W. R. Wadt and P. J. Hay, *J. Chem. Phys.* 1985, **82**, 270.

31   J. X. Wang, C. Li and H. Tian, *Coord. Chem. Rev.*, 2021, **427**, 213579.